ESTIMATION OF OUTLET MASS FLOW FOR A MONO-TUBE CAVITY RECEIVER FOR DIRECT STEAM GENERATION

José Zapata[1] and John Pye[2] and Greg Burgess[3]

[1] BEng(hons), PhD student, Research School of Engineering (RSE), Australian National University (ANU), Canberra, ACT 0200 Australia, phone +61-2-61253072, jose.zapata@anu.edu.au

[2] BE/BSc, PhD, Lecturer, RSE, ANU. [3] BSc (Hons), MappSc, Research Officer, RSE, ANU.

Abstract

This paper presents recent developments on a dynamic model for a mono-tube cavity receiver for direct steam generation with large scale parabolic dishes. Simulations of the model show that it is possible to assume a homogeneous distribution of heat flux along the receiver pipe without loosing accuracy in the calculation of receiver outlet temperature. The model in its current state produces an estimation of mass flow at the outlet for transient changes in incoming energy and receiver mass charge based on measurements of outlet pressure and modelled fluid properties. Simulations show that this approach produces good agreement between simulated and measured receiver outlet temperatures, but it is not currently possible to model pressure fluctuations in the receiver tube. Experimental data form the SG4 500 m² dish at the ANU is used to simulate the receiver and validate the results of the model.

1 Introduction

Direct steam generation for electricity production using parabolic dish concentrators is actively being researched at the Australian National University (ANU). Solar thermal power plants using this technology are intended to be deployed in large arrays of parabolic dishes, where each collector contributes steam to a central steam-turbine power block. It is of interest to model the dynamic behaviour of the conversion of water to superheated steam within the receiver in each collector, for the control of steam outlet temperature for each receiver in the array.

This paper contains recent developments on a dynamic heat transfer model for a mono-tube steam cavity boiler, which has been presented in previous SolarPACES conferences [1, 2]. In particular, it presents a method to compute boiler outlet mass flow based on a combination of modelled and measured boiler parameters. TRNSYS 16 simulations of the dynamic model incorporating outlet mass flow calculations are compared against experimental runs with the SG4 500 m² dish at the ANU [3] .

2 Current state of transient receiver model

A transient model of the heat exchange in a mono-tube cavity receiver has been under development at the ANU. The objective of this model is to represent the dominant behaviour of the receiver outlet temperature with respect to incoming radiation, ambient temperature, feed-water mass flow, etc. This information will be used to develop closed loop temperature controllers by manipulating the feed-water mass flow.

2.1 Modelling Approach

The receiver model is derived from first principles of conservation of mass and energy in the receiver tube. In steady operation, water transitions from liquid to saturated water/vapour mixture and then to superheated steam in a single pass of the receiver tube. The modelled tube is partitioned into three regions of liquid, saturated and superheated flow. The boundaries that define the extent of each region are time variant, and as a result the relative size of each region changes with changes in energy flow. For each region, the model poses a balance of mass and energy of the fluid, as well as a balance of energy in the tube wall, that is a function of the fluid properties and the region length. This approach is termed a “moving-boundary” formulation of the receiver tube [4] .

This model considers two other flow conditions: the water in the receiver tube transitions from liquid to saturated water/vapour mixture and exits the receiver; and the receiver tube is flooded with liquid water (e.g. during start-up and very low insolation). The model also poses a moving-boundary formulation for these two flow conditions. The flow conditions are termed modes and thus mode '1' represents the liquid only condition, mode '1-2' represents the liquid inlet and saturated outlet condition and mode '1-2-3' represents the aforementioned three region condition of liquid at the inlet, transition to saturation and superheated at the outlet. The model implements a switching approach following work previously done for evaporators and chillers in refrigeration [5] , to dynamically switch between modes. Other combinations of regions are possible, but are not currently considered by the model as they do not eventuate in the current system configuration.

2.2 Single vs multiple pressure regions in the receiver model

The model in this study assumes that all regions in each mode are at the same pressure P, as opposed to different pressures for each region, as presented in [1] . Multiple pressure regions introduced more variables to the model (a total of 13 instead of 8 for this study). The extra variables incur additional computation costs and numerical instability issues that remain unsolved. Experimental measurements of the SG4 500 m^2 dish at ANU show that the pressure drop between receiver inlet and outlet is approximately 300 kPa over 212 m of tube when the outlet is 500 °C and 4500 kPa. This relatively small pressure drop and the reduction in complexity justify the assumption of uniform receiver pressure in this study.

2.3 The effect of flux distribution in the receiver model

The incoming flux distribution in the receiver has also been considered for the solution of the transient behaviour of the mono-tube cavity receiver. In [2] , a distribution of the incoming flux from the SG4 500 m^2 dish at ANU onto the cavity receiver was generated using OPTICAD 10 and compared with steady state temperature measurements along the receiver tube. It was found that more than 50% of the radiation intercepted by the receiver impacts the tube between 100m and 150m along the tube length and as a result, the greatest incremental gain in thermal energy of the fluid happens in this portion of the tube.

The influence of a non-uniform flux distribution on the mono-tube receiver model was investigated using TRNSYS simulations of the receiver. The receiver model was simulated with both an uniform flux distribution and the non-uniform distribution in Fig. 1 to compare the effect of the distributed flux on the model behaviour.

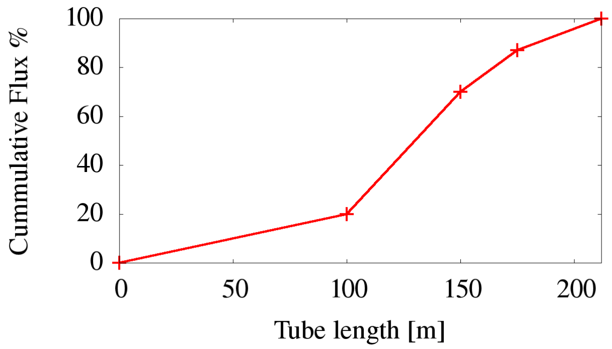

Fig. 1: Non-uniform flux profile in cumulative form used in comparison

The non-uniform flux profile influences the length of the fluid regions in the receiver model. When the flux per unit length is more intense, the fluid gains a certain amount of energy in a shorter span of receiver tube e.g. the tube will transition from saturated liquid to saturated vapour covering a shorter distance within the tube if the flux per unit length is more intense. Conversely, less intense flux will lengthen the fluid regions as they need to cover a larger area to capture a certain amount of heat energy.

A simulation that compares the effect of flux distribution on region lengths is shown on Fig. 2. Both versions of the model take data from an experimental run of the SG4 500 m^2 dish system that took place on the 18th of November 2011. Recorded data of feed-water mass flow, insolation, ambient temperatures and line pressures during this experimental run are fed to the receiver model, and the simulation calculates how the receiver model behaves under those circumstances.

The top graph shows the region lengths when a uniformly distributed flux is applied whereas the bottom graph shows the non-uniform flux distribution of Fig. 1. For each graph, consider the length of the receiver tube as the vertical axis with tube inlet represented at 0m and the outlet at 212m. The graph plots the location of the boundary between regions. The boundary between the liquid region and the saturated region in the model is at L_1 and the boundary between the saturated and the superheated region is at the modelled length L_1+L_2 . As the conditions on the simulation change (e.g. changes in feed-water mass flow or insolation) the boundaries will relocate, reflecting changes in region size and overall receiver energy.

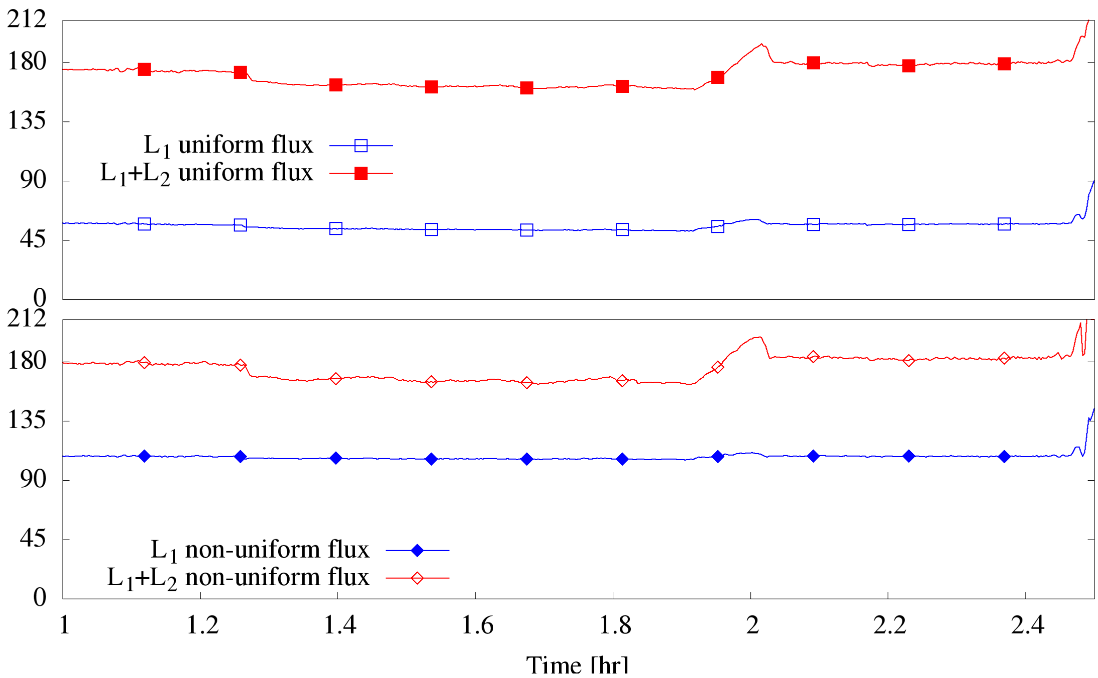

Fig. 2: Simulated region lengths for uniformly distributed flux (top) and non-uniform flux distribution (bottom)

Simulations in Fig. 2 show that the non-uniform flux distribution yields a shorter boiling region and a longer sub-cooled region than the uniformly distributed flux. This result is qualitatively consistent with experimental measurements presented in [2]. It has not been possible to obtain better agreement between simulated regions and the observation of region lengths in the receiver based on temperature as non-uniform flux distributions introduce numerical instability in the model, which is more severe as the flux distribution is more non-uniform. There is ongoing work by the authors to implement these simulations with more robust numerical integration algorithms.

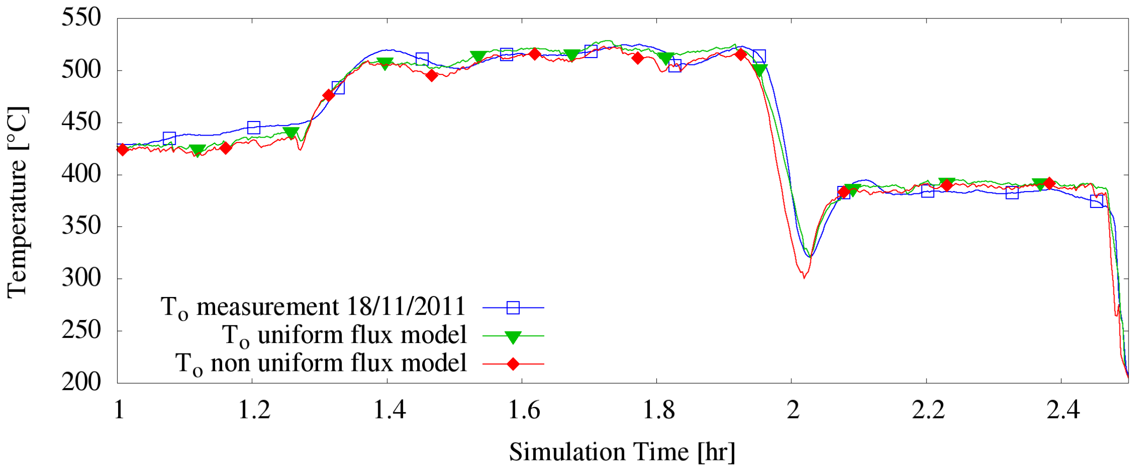

Fig. 3: Comparison of measured and simulated receiver outlet temperatures

The modelled outlet temperature in the receiver is not affected significantly by a non-uniform distribution. The receiver outlet temperature obtained in both the non-uniform and uniform flux distribution cases is compared to the measured receiver outlet temperature in Fig. 3. Both simulations show good agreement with the measured receiver outlet temperature under transients and steady periods. This indicates that both versions of the model agree on the total amount of energy absorbed by the fluid as it passes through the receiver. Furthermore, it shows that a uniformly distributed flux is adequate to represent the behaviour of the receiver outlet temperature, even though the fluid region lengths do not agree quantitatively with the boiling process in the mono-tube cavity receiver.

The receiver model in this study considers a uniformly distributed heat flux along the receiver tube length. This approach is preferred because it simpler, it has greater numerical stability than a non-uniform flux distribution and that the modelled receiver outlet temperature (i.e. the variable of interest for closed loop temperature control) shows comparatively good agreement with experimental measurements.

3 Outlet mass flow calculation

There is no available measurement of outlet mass flow at the ANU 500m² dish steam generation system and the measurement of two-phase mass flow and or quality remains difficult [6]. Receiver outlet fluid properties can be calculated by assuming $\dot{m}_o = \dot{m}_i$ whenever the receiver is in steady state and the fluid outlet is either liquid water or superheated steam. However this is not possible during transients or when the receiver outlet flow is a saturated water/vapour mixture. Thus there is a need to otherwise obtain the outlet mass flow for the receiver model. In this study, the mass flow at the receiver outlet is modelled from a momentum balance of the receiver tube.

3.1 Momentum balance on the receiver tube

Consider a simplified momentum balance along the entire receiver tube that includes the momentum flux carried into and out of the control volume by the fluid, the pressure forces at the tube ends and the shear friction force acted on the fluid by the tube.

$$\dot{m}_i \vec{v}_i - \dot{m}_o \vec{v}_o + A P_i - A P_o - \tau \pi D_i L = 0 \qquad (1)$$

This balance explicitly shows the outlet mass flow and connects it to other quantities within the receiver tube and its boundaries. The following assumptions about the fluid properties have been made to construct the momentum balance:

- The pressure drop profile in the receiver is assumed linear with tube length, and furthermore the pressure *P* is both the average receiver tube pressure and the pressure of the saturated region, therefore:

$$P = \frac{(P_i + P_o)}{2} \rightarrow P_i = 2P - P_o \tag{2}$$

- The shear stress τ is constant and uniform along the inner surface of the receiver tube.
- The mass inventory in the receiver is quantified by an averaged receiver density as follows:

$$\bar{\rho} = \begin{cases} \rho_1 & \text{if mode '1'} \\ (\rho_1 L_1 + \rho_2 L_2)\frac{1}{L} & \text{if mode '1-2'} \\ (\rho_1 L_1 + \rho_2 L_2 + \rho_3 L_3)\frac{1}{L} & \text{if mode '1-2-3'} \end{cases} \tag{3}$$

- Fluid velocities at the receiver inlet and outlet are approximated to mass flows at the inlet and outlet and connected to the mass inventory in the receiver by:

$$\vec{v}_i = \frac{\dot{m}_i}{\bar{\rho} A} \quad \text{and} \quad \vec{v}_o = \frac{\dot{m}_o}{\bar{\rho} A} \tag{4}$$

If the inlet pressure P_i in (2) and the fluid velocity expressions in (4) are substituted in the momentum equation (1), they can be rearranged to produce the following expression for the outlet mass flow in the receiver:

$$\dot{m}_o = \sqrt{\dot{m}_{\text{in}}^2 + 2\bar{\rho} A^2 (P - P_o) - \bar{\rho} A \tau \pi D_i L} \tag{5}$$

This expression connects the receiver outlet mass flow with the feed-water mass flow entering the receiver, the average receiver pressure *P*, the mass inventory in the receiver and the shear friction force in the receiver tube. In equilibrium, the average pressure in the receiver model balances against the pressure drop caused by shear along the receiver tube. This causes the outlet mass flow to equal the inlet mass flow in equation (5).

The value of $\dot{m}_o$ is calculated at each time step of the simulation and it is fed directly into the energy and mass balances in the receiver model. If the calculated value of the outlet mass flow differs from the feed-water mass flow (e.g. during transients), this will change the mass and energy inventory in the receiver. This feature is valuable when simulating start-up transients in the system, where the mass inventory changes from a receiver tube flooded with water to a receiver that is partially occupied with saturated and superheated steam. Simulations that demonstrate this effect are shown in section 4.

3.2 Modified expression for mode '1-2-3'

The estimation expression (5) provides useful results for the simulation of the receiver when the flow is modes '1' and '1-2'. In mode '1-2-3', the mass flow calculation can lead to disagreement between modelled and measured receiver outlet temperatures.

The outlet temperature in the receiver model is calculated from steam tables a function of the measured outlet pressure P_o and the modelled outlet enthalpy h_o . At the same time, the outlet mass flow is explicitly dependent on P_o and it is linked to the amount of energy leaving the receiver with the fluid by the term $\dot{m}_o h_o$. Fluctuations in P_o can therefore alter the mass and energy balance in the receiver model and overestimate changes in h_o , causing a significant departure between measured and modelled outlet temperatures. There lies the need to modify the estimation of outlet mass flow so that the model is less susceptible to changes in pressure in the system.

The mass flow estimation is modified in mode '1-2-3' by a damping coefficient k_m , which artificially reduced the influence of the pressure drop and shear stress terms on the estimation:

$$\dot{m}_o = \sqrt{\dot{m}_{\text{in}}^2 + k_m (2\bar{\rho} A^2 (P - P_o) - \bar{\rho} A \tau \pi D_i L)} \tag{6}$$

The damping coefficient is chosen arbitrarily to force agreement between measured and modelled receiver outlet temperatures. The simulations in this study use a value for the damping factor of $k_m = 0.01$.

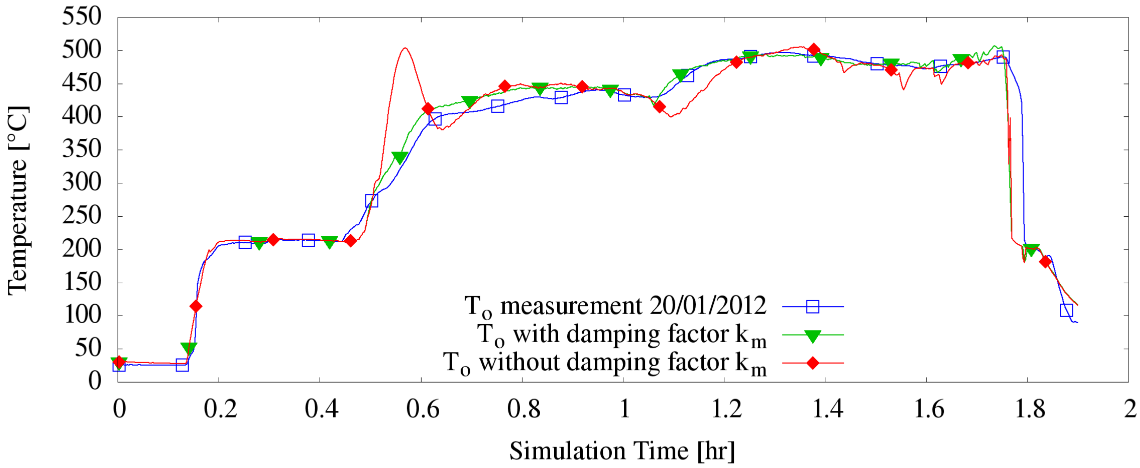

Fig. 4: Comparison of modelled and measured receiver outlet temperatures for experimental run of the SG4 500m² dish system on the 20th of January 2012.

This approach is simple and simulations show that it improves the prediction of receiver outlet temperatures. However, it does not give insight into the physical process governing the interaction between the mass inventory in the receiver and the changes in pressure downstream. Further research efforts in this area are aimed at improving the formulation of the momentum balance in the receiver tube.

4 Simulations

The receiver model, in conjunction with the outlet mass flow estimation has been implemented in TRNSYS 16. Experimental data from the ANU 500m² receiver has been fed to the simulation to compare the model response with measurements from an experimental run of the system performed on the 20th of January 2012. The model was simulated both with and without the damping factor k_m. At each time step, the simulation

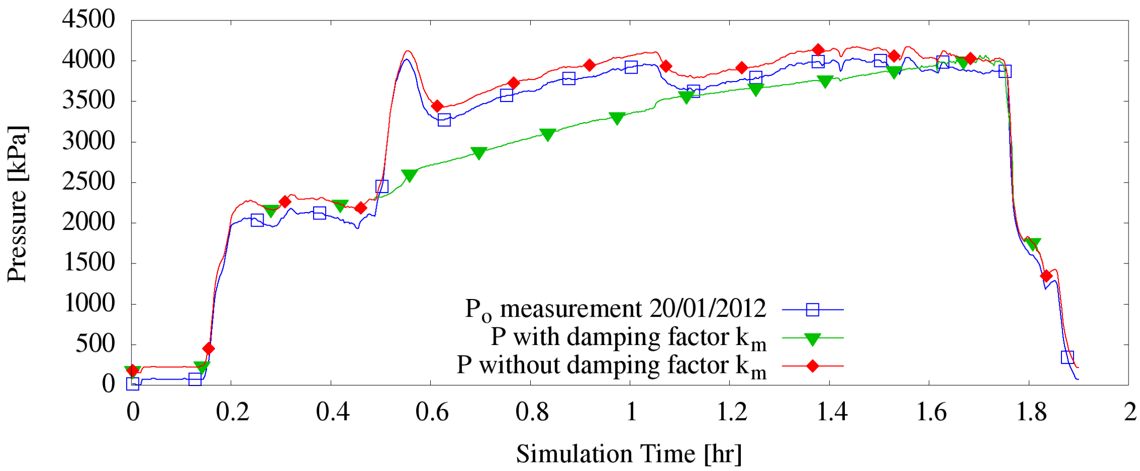

Fig. 5: Comparison of modelled receiver pressure and measured receiver outlet pressures for experimental run of the SG4 500m² dish system on the 20th of January 2012.

reads the following data: feed-water mass flow, temperature and pressure; insolation and ambient temperature; and receiver outlet pressure. The receiver model produces region lengths, mean pressure, outlet enthalpy, wall tube temperature for each region and the mean void fraction γ and their rates of change. In addition, the measured outlet temperature of the receiver has been included for comparison.

The receiver outlet temperatures in Fig. 4. show that in both cases, the receiver model can predict the onset of saturation and superheated temperatures in the receiver. Furthermore both versions of the model show good agreement with experimental results, when large transients are not included. In the case of large pressure transients (e.g. at 0.5hr and 1.1hr) the non-damped mass flow estimation results in departures between

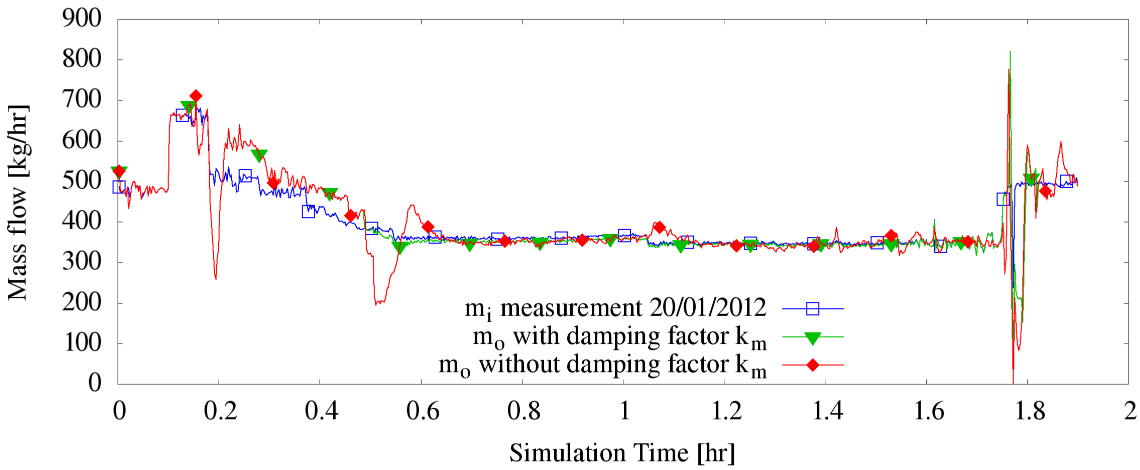

Fig. 6: Comparison of modelled and measured receiver outlet temperatures for experimental run of the SG4 500m² dish system on the 20th of January 2012.

modelled and measured outlet temperature.

Fig. 5 illustrates the trade-off of the damping factor. The measured outlet pressure P_o increases with the increase in the line pressure, as the fluid transitions to steam. At 0.55 h, there is a sudden change in line pressure when the system switches from the condenser to the steam engine, which increases the back pressure onto the receiver. At 1.1 h a valve that vents part of the steam to atmosphere downstream from the receiver is partly opened, and a similar effect is appreciated.

The receiver pressure in the model without damping surges and stays above the measured receiver outlet pressure, but this surge is affecting the calculation of receiver outlet enthalpy. When the damping factor is applied, the modelled receiver pressure P is much slower to track above the outlet pressure P_o .

The receiver pressure P is used in the calculation of fluid properties (e.g. densities, enthalpies, partial derivatives of properties with respect to pressure an enthalpy, etc) in each fluid region of the model. The damping factor is only applied in superheated output mode '1-2-3'. In particular, the calculated enthalpies of saturation are different between the two estimations, which results in slightly different size and location of the saturated region. As shown in section 2.3, this does not have a pronounced effect in the calculation of outlet temperature.

When going on an off sun, both versions of the models agree on large changes in receiver pressure. This indicates that the model is able to predict changes in pressure that are related to the changes in energy in the receiver (e.g. due to changes in radiation), but not when the line pressure is affected by external factors.

Outlet mass flow estimations with and without damping are compared against the feed-water mass flow measured for the experimental run in Fig. 6. During the start up period, both mass flow estimations calculate higher outlet flows than at inlet, in accordance with a discharge in the mass inventory in the receiver tube. Conversely, the outlet mass flow in both estimations is less than the feed-water flow during the shut-down period. During most of the simulation, both estimations agree, except during the external pressure transients mentioned above.

On the external pressure transient at 0.55 h, the non damped mass flow estimation oscillates with the change in pressure, which affect both the mass and energy balances in the receiver. The damped estimation follows the feed-water flow rate during this transient and thus the effect of external pressure fluctuations on the receiver mass balance is mitigated.

5 Conclusion

This paper has presented recent advances in the development of a control oriented model for the temperature response of a mono-tube cavity receiver for direct steam generation at the ANU.

The effects of pressure drop and incident heat flux distribution in the receiver tube have been considered against the complexity of incorporating these effects in a simulation. It has been found that neglecting the effects of pressure drop and flux distribution can improve the numerical stability of the model and without a large penalty on the calculation of temperature at the receiver outlet.

In addition, an estimation of receiver outlet mass flow has beep presented that uses both modelled and measured receiver quantities. The mass flow at the outlet is a boundary condition to the receiver model and therefore needed to solve the model equations. Simulations show that the outlet mass flow estimation is useful to predict the receiver outlet temperature under conditions obtained from the SG4 500 m^2 dish steam generation system at the ANU. It has been also shown that this estimation is sensitive to disturbances in receiver outlet pressure caused by factors external to the receiver. Future efforts to improve the model accuracy should focus on incorporating more physical effects on the receiver and system, but care must be taken to preserve the simplicity of this approach.

The receiver modelling approach and outlet mass flow estimation presented in this paper, has the potential to provide a tool to estimate the state of direct steam generation receivers for control purposes. Despite the simplifications incurred in their development, this approach results in a set of non-linear ordinary differential equations which can form the basis for state estimators and observers for systems of this type.

References

[1] J. Zapata, K. Lovegrove and J. Pye, 2010. 'Steam Receiver Models for Solar Dish Concentrators: Two Models Compared'. In *SolarPACES 2010 conference, Perpignan, France*, .

[2] J. Zapata, J. Pye and K. Lovegrove, 2011. 'Dynamic Simulation of Mono-tube Cavity Receivers for Direct Steam Generation'. In *SolarPACES 2011 conference, Granada, Spain*, .

[3] K. Lovegrove, G. Burgess and J. Pye, 2011. 'A new 500 m2 paraboloidal dish solar concentrator', *Solar Energy* **85**, 620 - 626.

[4] J. Jensen and H. Tummescheit, 2002. 'Moving Boundary Models for Dynamic Simulations of Two-Phase Flows'. In *Proc. of the 2nd Int. Modelica Conference*, .

[5] T. L. McKinley and A. G. Alleyne, 2008. 'An advanced nonlinear switched heat exchanger model for vapor compression cycles using the moving-boundary method', *International Journal of Refrigeration* **31**, 1253 - 1264.

[6] G.-B. Zheng, N.-D. Jin, X.-H. Jia, P.-J. Lv and X.-B. Liu, 2008. 'Gas–liquid two phase flow measurement method based on combination instrument of turbine flowmeter and conductance sensor', *International Journal of Multiphase Flow* **34**, 1031 - 1047.